EVIDENCE OF THARSIS-RADIAL DIKE INTRUSION IN SOUTHEAST ALBA PATERA FROM MOLA-BASED TOPOGRAPHY OF PIT CRATER CHAINS.

Chris H. Okubo[1] and Richard A. Schultz, Geomechanics–Rock Fracture Group, Department of Geological Sciences and Engineering /174, University of Nevada, Reno, NV, 89557-0138. [1]chriso@mines.unr.edu

INTRODUCTION: Tharsis-radial graben and pit crater chains (catenae) have been interpreted as the result of igneous dike intrusions [1,2,3], which attain lengths in excess of 2000 km from the center of the Tharsis volcano–tectonic province. Based on the assumption that these Tharsis–radial graben and pit crater chains are underlain by dikes, geodynamic models of lithospheric uplift have been proposed to account for the stress state required for Tharsis–radial dike propagation [4] and the attendant magma fluxes have been estimated [2].

In this abstract, we test the fundamental assumption that Tharsis–radial pit crater chains are underlain by igneous dikes by examining Phlegethon, Acheron and Tractus Catenae on the southeast flank of Alba Patera. Following [5] we compare MOLA–based topography against standard numerical model predictions of surface deformation above buried and surface–breaking dikes and normal faults. We find that these pit crater chains have local cross–strike topographies that are consistent with origins by either dike intrusion, by normal faulting, or by a mixed–mode of dike intrusion and normal faulting, with the causative tendencies changing with position along strike of each pit crater chain (Fig. 1).

CHARACTERISTIC FAULT– AND DIKE–INDUCED TOPOGRAPHY: We employ a boundary element code [6] to establish the distinct topographic characteristics of surface–breaking and buried normal faults and dikes under natural variations in crustal strength and deformability. We vary crustal elastic modulus between 1 GPa and 60 GPa, Poisson's ratio between 0.2 and 0.3, and the σ_3 to σ_1 principal stress ratio (a function of friction, cohesion and groundwater condition) between 3 and 5, with σ_1 equal to lithostatic load. The average magma to crustal density ratio is 0.85. The modeled normal faults are planar and dip at 50° to 70°, and dikes dip at 70° to 90°.

Pertinent results from this series of models are shown in figure 2. Through the range of tested strength and deformability parameters, the topography above a vertical dike is characteristically symmetric, while asymmetric topography is predicted above inclined dikes. The uplifted ridges on either side of the modeled dike tops have a concave-down topography. The topography around a single normal fault is shown to be characteristically asymmetric, and [5] has shown that this asymmetry can also be predicted when an antithetic fault is present within the hanging wall. The uplifted footwall is characterized by concave–up topography, while the subsided hanging wall has a characteristic concave–down topography.

EVALUATION OF OBSERVED CATENA TOPOGRAPHY: The topography of Phlegethon, Acheron and Tractus Catenae are characterized using high–resolution MOLA–based digital elevation models (DEMs). A series of discontinuous–surface DEMs are constructed of these catena following the procedure of [7] for a nearneighbor grid. These DEMs are constructed with a 200 pixel per degree (~296 m/pixel) spatial resolution. Individual DEM pixels are defined as the average value of all MOLA elevations that fall within that pixel, with no interpolation made across pixels that lack MOLA data. Topographic profiles are extracted from these DEMs through

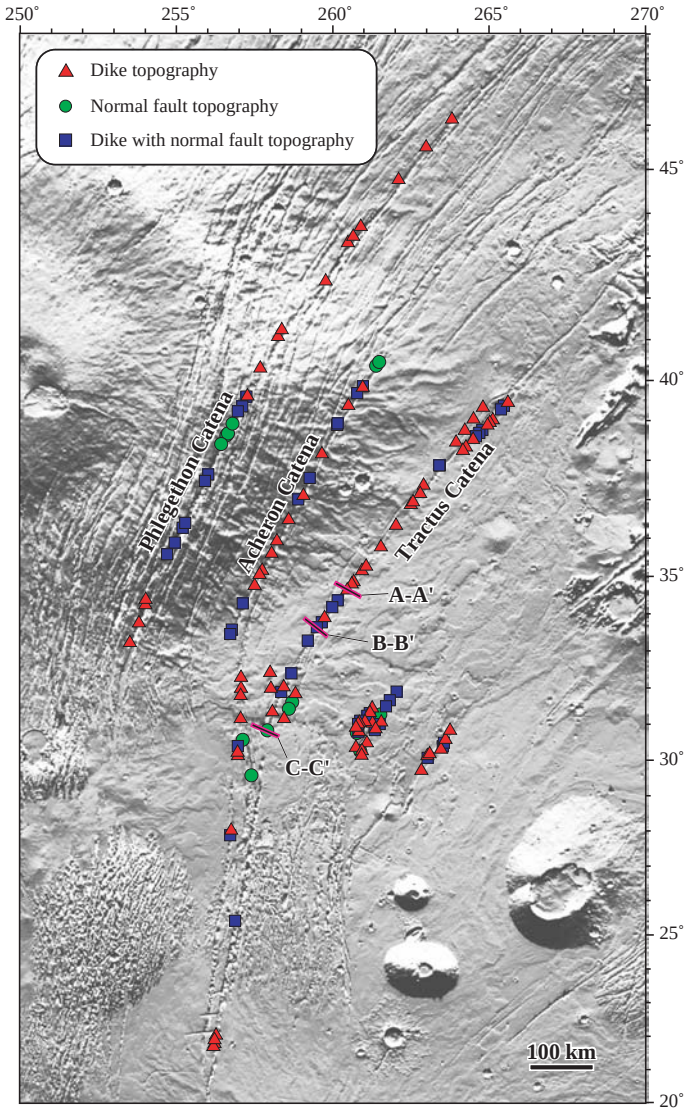

Figure 1. Distribution of topographic classifications along pit crater chains in southeast Alba Patera. Labeled profiles refer to figure 3. Base map is MOLA shaded relief, with illumination from the north.

contiguous MOLA–based pixels that span pit chain terminations, pit craters and septa between pit craters.

Profiles are classified as dike-related where there is a pair of concave–down ridges of sub–equal peak elevation on either side of the catena (Fig. 3). 'Mixed–mode' topographies are also observed, where the paired concave–down ridges characteristic of dike–related topography have offset peak elevations. Mixed–mode topography is attributed to either normal fault displacements along inclined dikes, or dike propagation along preexisting normal faults. Profiles are classified as normal fault–related where there is a vertical offset across the catena and dike–like concave–down ridges are not observed.

Our analysis reveals distinct clusters of dike–related, normal fault–related and mixed–mode topographies (Fig. 1). At Phlegethon Catena, dike–related topography is dominant around both lateral tips. Normal fault-related topography is

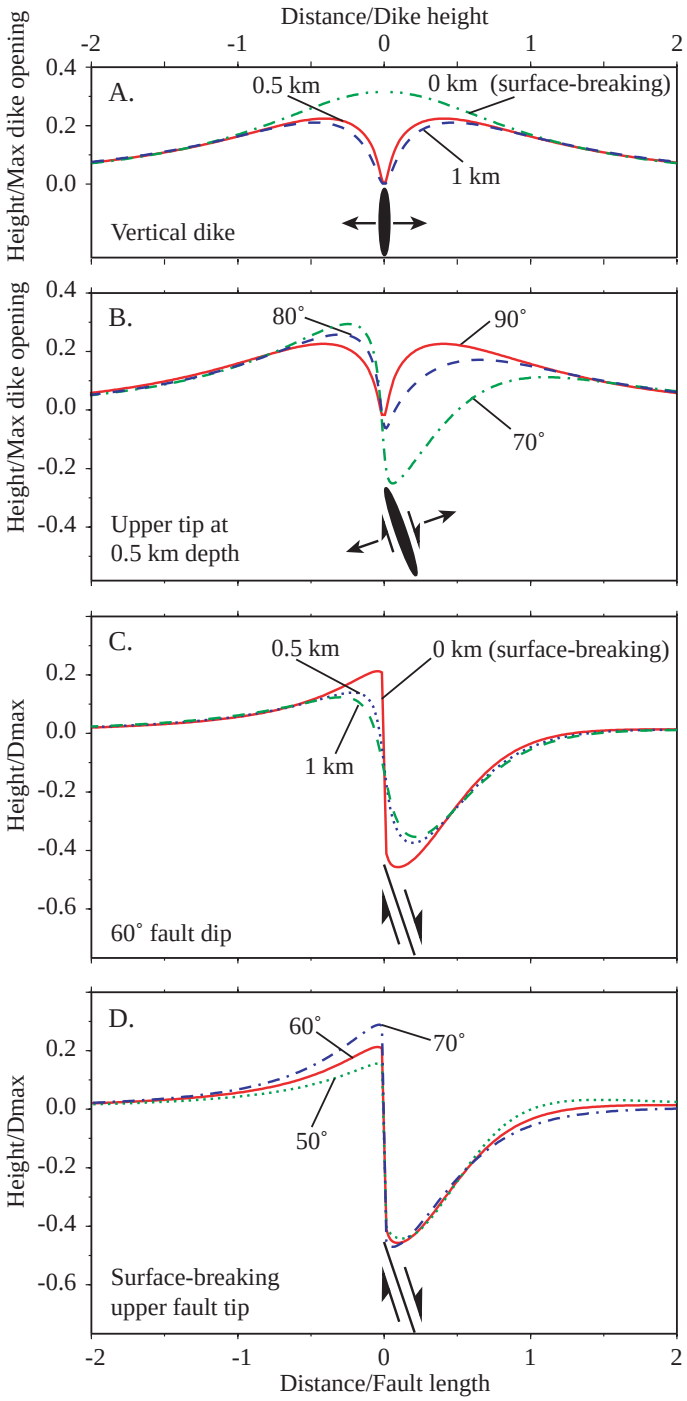

Figure 2. Model–predicted topography above A) vertical dikes with different upper tip depths, B) dikes at different dip angles, C) normal faults at different upper tip depths, and C) normal faults at different dip angles. In C) and D) Dmax is the maximum fault displacement.

dominant in the midsection and zones of mixed–mode topography occurs between this midsection and the lateral tips.

The topography of Acheron Catena is characterized by normal fault topography at its northern–most tip and by mixed–mode and dike–related topography along the remainder of its length. At Tractus Catena, mixed–mode topography is common along its northern tip and at its intersection with a strand of pit craters trending toward Acheron Catena. At this intersection, normal fault topography is also observed, while the midsection of Acheron is dominated by dike-related topography.

Conclusions and Implications: We find that the MOLA–based topography of Phlegethon, Acheron and Tractus Catenae is consistent with origins by both causative normal faulting and dike intrusion and that the apparent causative mechanism changes with position along strike of each pit chain. This spatial juxtaposition of causative processes suggests that either Tharsis–radial dikes intruded along pre-existing normal faults, or that a normal sense of displacement occurred along inclined dikes. Pit crater formation would have then occurred during propagation of these dikes [e.g. 8] or possibly occurred during normal fault growth [e.g. 9]. Additional discussion on this topic is also provided in a companion abstract [Okubo and Schultz, *this volume*].

Results of this analysis provide quantitative evidence that the Tharsis–radial pit crater chains in southeast Alba Patera (Phlegethon, Acheron and Tractus Catenae) overlie causative dikes. This finding substantiates interpretations of Tharsis–radial dikes in the region [1,3], and thereby supports geodynamic models of lithospheric uplift by mantle plumes below Tharsis [2,4]. These results are also entirely consistent with models of lithospheric flexure by Tharsis loading [11,12], which predict maximum horizontal compressive stress directions radial to the center of Tharsis, which are necessary for Tharsis-radial dike propagation.

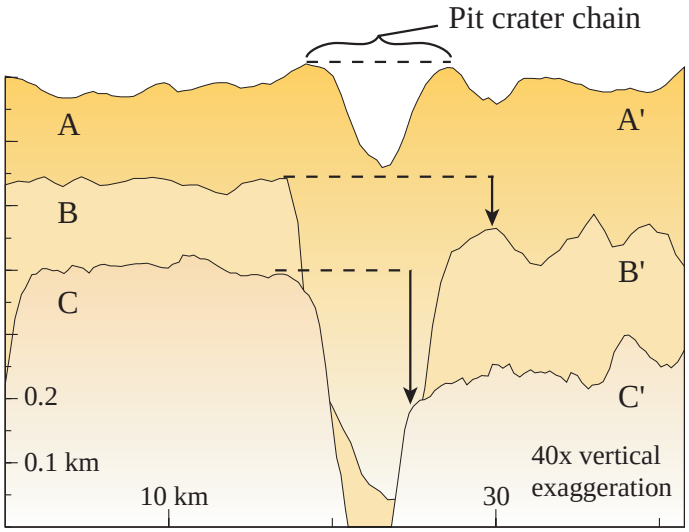

Figure 3. Examples of MOLA-based topography across Tractus Catena showing A–A') symmetric ridges of dike–related topography, B–B') offset ridges of mixed-mode topography, and C–C') surface offset of normal fault–related topography. See figure 1 for profile locations.

References: [1] Ernst et al., (2001) *Annu. Rev. Earth Planet. Sci*., 29, 489–534. [2] Wilson and Head, (2002) *J. Geophys. Res*., 2001JE001593. [3] Mège et al (2003) *J. Geophys. Res*., 2002JE001852. [4] Mège et al., (1996) *Annu. Rev. Earth Planet. Sci*., 44, 1499–1546. [5] Schultz et al., (2004) *Geology*, 32, 889–892. [6] Schultz, (1992) *Eng. Anal. Bound. Elem.*, 10, 147–154. [7] Okubo and Schultz, (2004) *Comp. Geosci*., 30, 59–72. [8] Okubo and Martel (1998), *J. Volcanol. Geotherm. Res*., 86, 1–18. [9] Wyrick et al., (2004) *J. Geophys. Res*., 2004JE002240. [11] Solomon and Head, (1982) *J. Geophys. Res*., 87, 9755–9774. [12] Banerdt et al., (1992) in *Mars*, 249–297, Univ. Ariz. Press.

Abstract published in: Lunar and Planetary Science XXXVI, CD-ROM, Lunar and Planetary Institute, Houston (2005).